

ADAPTIVE WAVELET-BASED FAMILY TREE QUANTIZATION FOR DIGITAL IMAGE WATERMARKING

Boyd McKinnon and Xiaojun Qi
Computer Science Department
Utah State University
Logan, UT 84322-4205
bkm@cc.usu.edu and xqi@cc.usu.edu

ABSTRACT

This paper presents an adaptive wavelet-based blind digital watermarking scheme for copyright protection. The wavelet coefficients in the same spatial directions at different decomposition levels are grouped into family trees. The watermark is embedded by quantizing the family trees. The trees are adaptively quantized using the characteristics of the human visual system in the wavelet domain so the maximum allowable changes can be made to the original image without any visible distortions. In the meantime, the quantized trees exhibit a large enough difference for blind watermark extraction. Experimental results demonstrate that the proposed system achieves comparable performance as the fixed quantization approach. Specifically, the proposed system is robust against common image processing attacks and more resistant to the compression attacks than the fixed quantization approach.

KEY WORDS

Human visual system, tree quantization, family tree, and wavelet transform

1. Introduction

Claims to ownership within the digital world are a hot topic since the need to prove ownership of intellectual knowledge or digital media is becoming more necessary. To solve this problem, individuals have begun to create watermarks similar to those that are located on a fine quality paper or on U.S. currency. However, digital watermarks are different from paper watermarks in terms of visibility. That is, paper watermarks are visible to everyone who knows how to look for them. Digital watermarks are invisible and the various media for storing the watermarks are not visibly altered either. As a result, others may be unaware that the watermark is even present. However, an appropriate watermark detection method must be available to indicate whether a watermark is embedded in the media and therefore prove the ownership.

The techniques for creating the invisible watermarks have been improved over the past decade. In general, they all address the following key issues: (1) the limitation of visual distortion, (2) the ability to retrieve the original digital media, (3) accurate detection, and (4) robustness against any intentional or unintentional attacks which may ruin the watermark [1, 2]. It is also widely accepted that robust watermarking techniques should largely exploit the characteristics of the human visual system (HVS) [3-5]. In addition, a blind watermarking technique [6] is preferred since an unmarked original is not needed for the detection process.

In this paper, we will utilize the characteristics of the HVS to construct a blind watermarking scheme for images. This scheme effectively combines the advantages of the quantization and the discrete wavelet transform (DWT) for more effectively hiding a robust watermark. Three categories of related algorithms are briefly reviewed here.

The first category directly adds pseudo-random watermark sequences to the wavelet domain using multiplicative or additive schemes. For example, Cox *et al.* [7] embed a set of independent Gaussian distributed sequences into the perceptually most significant frequency components of DWT of the images. Wang *et al.* [8] embed the weighted watermark determined by a subband-dependent value in the most significant DWT coefficients. Barni *et al.* [9] use a pixel-wise mask to take into account the texture and the luminance content of all image subbands. The watermark is adaptively added to the corresponding largest detail bands determined by the pixel-wise mask without any perceived quality degradation of the image.

The second category hides binary or gray-scale logos in the wavelet domain using multiplicative or additive schemes. Both the binary/gray-scale logo and the original image are hierarchically decomposed by DWT. In [10], the scaled binary logo is repeatedly added to the DWT decomposition of the image based on the noise sensibility in each small block. In [11], each detail subband of the logo is embedded into the corresponding detail subband of the image based on the variance on a block-by-block basis. Hsieh *et al.* [12] adaptively embed the original

logo in the qualified significant wavelet trees to achieve the robustness of the watermarking. However, the original image is needed for watermark detection in both [11] and [12].

The third category embeds pseudo-random watermark sequences in the wavelet domain using quantization techniques. Kundur and Hatzinakos [13] embed each watermark bit by quantizing a single wavelet coefficient out of a set of coefficients corresponding to a particular spatial region. Wang and Lin [14] embed each watermark bit by quantizing super trees. The quantized super trees exhibit a large enough statistical difference and therefore will be used for watermark extraction. However, both methods require extensive experiments to decide the appropriate quantization threshold without degrading the original image.

In this paper, we develop a robust watermarking scheme which achieves the image authentication under various attacks including image compression, scaling, histogram equalization, multiple watermarks, etc. The parent-child relationship in wavelet decompositions is explored to construct family trees. Similarly, this relationship is further utilized to determine the maximum amount of changes before the human eyes can detect a difference using the HVS model [15]. This determined maximum amount of changes is then used to automatically determine the quantization index for each family tree. The proposed watermarking scheme embeds and detects each watermark bit by quantizing the family trees using the automatically determined quantization index. The remainder of the paper is organized as follows:

- Section 2 introduces several concepts related to our proposed technique and details the proposed embedding procedure.
- Section 3 presents the proposed watermark extraction and detection scheme.
- Section 4 shows the experimental results.
- Section 5 draws conclusions.

2. Watermark Embedding Process

2.1 Several concepts

We will introduce several concepts used in the proposed watermarking scheme.

A. Family Tree and Quantization Index q_n

A family tree is constructed by grouping three levels of wavelet coefficients in the same spatial directions. Fig. 1 illustrates such groupings of the wavelet coefficients in the horizontal, vertical, and diagonal directions. Specifically, the root of a family tree is a wavelet coefficient in one of the three highest frequency subbands marked as $C_{4,1}$, $C_{4,2}$, and $C_{4,3}$, where $C_{i,j}$'s indicates the wavelet coefficients in the i th decomposition level along j direction ($j=1$ denotes horizontal direction, $j=2$ denotes

vertical direction, and $j=3$ denotes diagonal direction). Its four direct children are the ones located along the same spatial directions in the second highest frequency subbands (i.e., $i = 3$). Each of the four children has their four corresponding children located along the same spatial directions in the third highest frequency subbands (i.e., $i = 2$). Consequently, each family tree contains 21 coefficients, namely, 1 ancestor coefficient from $C_{4,j}$, 4 children coefficients from $C_{3,j}$, and 16 grandchildren coefficients from $C_{2,j}$ where $j = 1, 2, \text{ or } 3$. For an image of size 512 by 512, there are a total of $3 * 32^2 = 3072$ family trees.

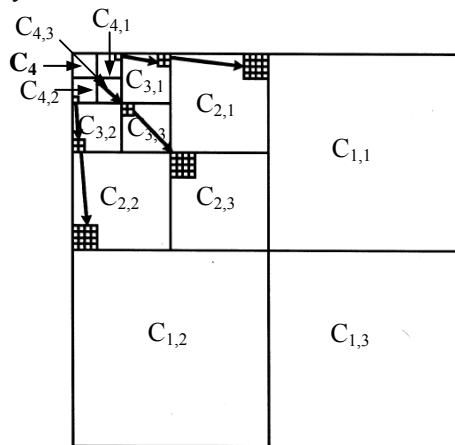


Fig. 1: Illustration of the construction of three family trees using wavelet coefficients along the same spatial direction (i.e., horizontal, vertical, and diagonal)

In our proposed watermark system, an array is used to store each member of the family tree in the order of ancestor, children, and grandchildren. Fig. 2 shows such a storage structure together with the quantization index q_n which indicates the bit planes to be quantized for each wavelet coefficient in a pair of family trees. The quantized bits are discarded (i.e., set to 0's) and are shown in the shady areas in Fig. 2. The position of q_n is determined from the maximum allowable error of two pairs of compatible family tree pair, which will be discussed in section 2.2. In other words, q_n is the furthest position from the bottom within the compatible family tree pair where the quantization error is less than the maximum allowable error if all values below it as shown in the shady areas in Fig. 2 are set to 0's.

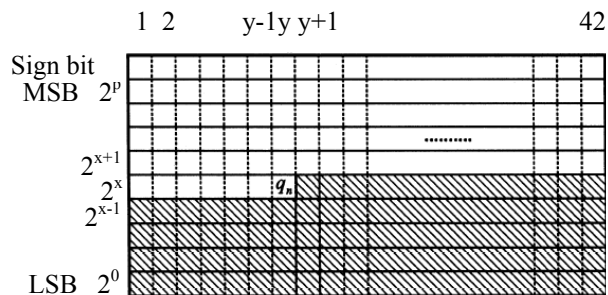


Fig. 2: Position of q_n within the Compatible Family Tree Pair

B. Human Visual System

Human visual system (HVS) models the sensitivity of the human eyes to the input signal (i.e., how our eyes observe invisibility). It is necessary to take the HVS into account when developing a watermarking system so that visual distortion will be kept to minimum and the watermarking methods are optimized. In our proposed system, we utilize DWT as a channel to exploit the HVS iso- and near-frequency masking effect. Such a choice is mainly because DWT has the excellent spatio-frequency localization property and has been extensively utilized to identify the image areas where a disturbance can be more easily hidden.

Three HVS-based considerations include [15]:

- The eyes are less sensitive to noise in high-resolution bands and in those bands having orientation of 45° (i.e., $j=3$ in our illustration).
- The eyes are less sensitive to noise in the areas where brightness is high or low.
- The eyes are less sensitive to noise in highly textured areas but, among these, more sensitive near the edges.

These three HVS-based characteristics will be integrated into our system to find the appropriate quantization without bring up any distortion.

C. HVS-based Maximum Allowable Change

The HVS-based maximum allowable change corresponds to a maximum change for a wavelet coefficient so no visible changes to the original image can be detected by human eyes.

The maximum allowable change to each wavelet coefficient at location (x, y) in the i th decomposition level along j direction can be computed as the weighted product of three items:

$$q_i^j(x, y) = A(i, j)B(i, x, y)C(i, x, y)^{0.2} / 2 \quad (1)$$

where $i=1, 2, 3, 4$ and $j=1, 2, 3$. Each of the three items is explained as follows:

- $A(i, j)$ denotes the sensitivity of the human eyes to noise changes and is computed as:

$$A(i, j) = \begin{cases} 1.00 & \text{if } i=1 \\ \sqrt{2} & \text{if } j=3 \\ 1 & \text{if } j=1,2 \end{cases} \times \begin{cases} 0.32 & \text{if } i=2 \\ 0.16 & \text{if } i=3 \\ 0.10 & \text{if } i=4 \end{cases} \quad (2)$$

- $B(i, x, y)$ denotes the sensitivity of the human eyes to local brightness or darkness and is computed as:

$$B(i, x, y) = 1 + L'(i, x, y) \quad (3)$$

where

$$L'(i, x, y) = \begin{cases} 1 - L(i, x, y) & \text{if } L(i, x, y) < 0.5 \\ L(i, x, y) & \text{otherwise} \end{cases},$$

$$L(i, x, y) = \frac{1}{256} C_4 \left(1 + \left\lfloor \frac{x}{2^{5-i}} \right\rfloor + \left\lfloor \frac{y}{2^{5-i}} \right\rfloor \right),$$

C_4 are the detail wavelet coefficients, and i corresponds

to the wavelet decomposition levels (i.e., $i = 1, 2, 3, \text{ and } 4$).

- $C(i, x, y)$ denotes the sensitivity of the human eyes to the texture activity in the neighbourhood of the pixel.

$$C(i, x, y) = \sum_{k=1}^{5-i} \frac{1}{16^{k-1}} \sum_{j=1}^3 \sum_{x'=1}^2 \sum_{y'=1}^2 \left[C_{k+i-1}^j \left(y' + \frac{x}{2^{k-1}}, x' + \frac{y}{2^{k-1}} \right) \right]^2 \times \text{Var} \left\{ C_4 \left(1 + y' + \frac{x}{2^{5-i}}, 1 + x' + \frac{y}{2^{5-i}} \right) \right\}_{x'=1,2 \text{ and } y'=1,2} \quad (4)$$

This maximum allowable error will be used in our proposed watermarking scheme to automatically determine the maximum quantization index of each family tree to ensure that there is no visible distortion to the original image.

2.2 Embedding steps

The detailed embedding process is as follows:

1. Perform a four level DWT decomposition upon the original image and locate all the family trees.
2. Compute the maximum allowable change for each family tree. The computation is first performed on all the grandchildren wavelet coefficients in the family tree using (1). That is, calculate the maximum allowable changes for all the grandchildren wavelet coefficients using (1). The final maximum allowable change for each family tree is then computed as the average of all these maximum allowable changes.
3. Construct pairs of compatible family trees (CFTs) using a private key based random sequence. Two family trees are compatible if the difference between the maximum allowable changes of two family trees is less than 150.
4. Compute the maximum allowable change for each pair of CFTs by averaging the two maximum allowable changes of the two compatible family trees.
5. Generate a pseudo-random watermark sequence of 1's and -1's with the length equal to the half of the number of pairs of CFTs using a private seed.
6. Sequentially pair each watermark bit W_i with two pairs of CFTs ($T_{i,1}, T_{i,2}$) and embed the watermark bit in the following manner:
 - 6.1 Compute the maximum allowable quantization error Q_i as one third of the averaged maximum allowable changes of $T_{i,1}$ and $T_{i,2}$.
 - 6.2 Locate the $q_{n,1}$ for $T_{i,1}$ based on Q_i .
 - 6.3 Locate the $q_{n,2}$ for $T_{i,2}$ based on Q_i .
 - 6.4 If $W_i = -1$, $T_{i,1}$ will be chosen for embedding.
 - 6.5 If $W_i = 1$, $T_{i,2}$ will be chosen for embedding.
 - 6.6 The chosen compatible family tree pair $T_{i,1}$ or $T_{i,2}$ will be quantized using $\max(q_{n,1}, q_{n,2})$.

7. Perform a four level inverse DWT on the quantized wavelet coefficients to construct the watermarked image.

3. Watermark Detection Process

The first five steps of the watermark detection process are the same as the ones of the watermark embedding process. Based on the sequentially paired two pairs of CFTs ($T'_{i,1}$, $T'_{i,2}$), the watermark extraction step is as follows:

1. Compute the maximum allowable quantization error Q'_i as one third of the averaged maximum allowable changes of $T'_{i,1}$ and $T'_{i,2}$.
2. Locate the $q'_{n,1}$ for $T'_{i,1}$ based on Q'_i .
3. Locate the $q'_{n,2}$ for $T'_{i,2}$ based on Q'_i .
4. If $q'_{n,1} > q'_{n,2}$, $W'_i = -1$. Otherwise, $W'_i = 1$.

The extracted watermark sequence W' is further compared with the original watermark sequence W to determine the presence of the watermark in the probe image. In specific, the normalized correlation coefficient is computed:

$$\rho(W, W') = \frac{\sum_i W_i W'_i}{N} \quad (5)$$

where W_i and W'_i are the i th bits of the original and extracted watermarks and N is the length of the watermark sequence. This normalized correlation coefficient is further compared with a threshold P_T to determine the presence of the watermark. That is: if $\rho(W, W') \geq P_T$, we claim the existence of the watermark. Otherwise, we claim that there is no watermark in the probe image.

The choice of the P_T is based on the false positive error P_{fp} , the probability of W_i unequal to W'_i (i.e., P_e), and the length of the watermark sequence (i.e., N). Such a relation can be express by [13]:

$$P_{fp} = \sum_{k=(P_T+1)/2N}^N \binom{N}{k} P_e^{N-k} (1-P_e)^k \quad (6)$$

Let $N = 768$ (i.e., $3072/4$), which corresponds to the maximum number of pairs of the CFT pair. For $P_T = 0.15, 0.20$, and 0.25 , the corresponding P_{fp} is 1.61×10^{-5} , 1.5×10^{-8} , and 2.14×10^{-13} , respectively. Consequently, given a false positive probability, we can choose an appropriate P_T to meet the requirement. In our proposed watermarking scheme, we set this threshold as 0.15 , which will give a 1.61×10^{-5} chance of a false positive when the watermark length is 768 bits long.

4. Experimental Results

To evaluate the performance of the proposed watermarking scheme, a variety of experiments have been performed to test on images with distinct textures using different kinds of attempting attacks.

4.1 Watermark Invisibility

The watermark invisibility is shown in Fig. 3. It clearly shows that there is no obvious visual distortion in watermarked images by using adaptive wavelet-based family tree quantization technique (i.e., our proposed approach) and the fixed wavelet-based quantization technique [14]. Based on the PSNR values, we conclude that our HVS-based adaptive embedding scheme allows stronger changes on the host image than the fixed embedding scheme where the fixed maximum allowable quantization error is set to be 100.



Fig. 3: The Invisibility in the Watermarked Images

- (a) Original Image
- (b) Adaptive Embedding: PSNR = 40.40 db
- (c) Fixed Embedding: PSNR = 42.75 db

4.2 Simulation Results

Simulations for different attacks including scaling, histogram equalization, compression, multi-marking, and the like have been performed. In specific, we compare the performance of our proposed watermarking scheme with our implemented version of the quantization approach [14].

A. Simulation Results on Undisturbed Watermark Results

Table 1 shows the average PSNR values and the normalized correlation coefficients (ρ 's) using 12 different private keys for generating the pairs of CFTs for both our approach and the quantization approach [14]. It clearly shows that both methods have high detection probabilities and high PSNRs above 35 dB. That is, we are able to successfully retrieve the watermark that was embedded on all kinds of textured images since the ρ values of both approaches are higher than the threshold of 0.15.

Table 1: Averaged Undisturbed Test Results

	Our Approach		Fixed Quantization	
	PSNR	ρ	PSNR	ρ
Baboon	47.52	1.0	49.69	1.0
Peppers	46.77	0.99	48.11	1.0
Lena	40.40	0.96	42.75	0.97
Elaine	47.13	1.0	49.49	1.0
Boat	46.93	1.0	48.46	1.0
Goldhill	48.14	0.99	47.95	0.99

B. Simulation Results on Scaling and Histogram Equalization Attacks

Different scaling ratios have been performed on the probe images to test the robustness of the proposed approach. Table 2 shows the averaged rescaling tests on six images. It demonstrates that both methods are able to detect their watermarks after the images were rescaled. However, our normalized correlation coefficients are smaller. Similarly, both approaches successfully resist the histogram equalization operation.

Table 2: Averaged Rescaling Test Results and Histogram Equalization Results

	Our Approach		Fixed Quantization	
	Scaled 0-255	Histogram Equalization	Scaled 0-255	Histogram Equalization
Baboon	0.66	0.45	0.67	0.28
Peppers	0.99	0.68	1.00	0.75
Lena	0.79	0.47	0.93	0.66
Elaine	0.99	0.79	1.00	0.75
Boat	0.99	0.59	0.99	0.48
Goldhill	0.93	0.43	0.97	0.51

C. Simulation Results on Compression Attacks

Fig. 4 summarizes the simulation results of both methods under the JPEG compression with a quality factor of 10% and higher. In Fig. 4, QT indicates the approach proposed in [14] and DTQ indicates our proposed approach. The test results convey that both approaches can handle a JPEG compression with a quality factor of 40% and higher since the probability of detection is greater than 15%. However, our normalized correlation coefficients are consistently higher. This indicates that the proposed approach is more robust against the compression attacks.

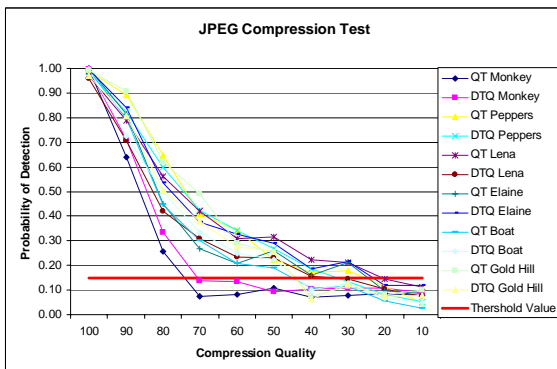


Fig. 4: Compression Test Results

D. Simulation Results on Multi-watermarking Attacks

We also test the robustness against over-watermarking or multi-marking an image. The watermark is first embedded into our test images with a private seed of 37. Four additional watermarks are then applied to the same image using different seed values ranging from 1 through 4. Table 3 lists the difference of the ρ values. It clearly shows that our approach is more robust against multi-watermarking attacks since the differences of the ρ values are quite large in all situations. In other words, we claim that the attackers would not be able to destroy our

watermark by embedding multiple watermarks of the same type into our watermarked image even if they know the type of watermarking technique we employed.

Table 3: Difference in Multi-Watermarking Results

	$(\rho \text{ of our approach}) - (\rho \text{ of approach in [14]})$			
	1	2	3	4
Baboon	0.40	0.67	0.75	0.80
Peppers	0.51	0.74	0.84	0.88
Lena	0.48	0.67	0.82	0.87
Elaine	0.43	0.68	0.78	0.89
Boat	0.47	0.72	0.85	0.85
Goldhill	0.43	0.68	0.76	0.81

E. Simulation Results on Other Attacks

We also performed different kinds of other attacks, including filter operations, pixel shifts, noise addition, bit-plane removal, and rotation, to test the performance of our proposed system. For the filter attacks, both methods perform about equal and neither stands out as more robust than the other. In the pixel-shifting tests, it is clear that our method performs worse than the fixed quantization method mainly due to the fact that the adaptively computed maximum quantization errors are sensitively to the shift operations. Both methods can handle “salt and pepper” noise and additive noise which does not cause major visual distortion within the image. Similarly, both methods have a resistance against bit-plane removal through the three lower (least significant) bit-planes. However, both methods fail to be robust against the rotation attacks.

5. Conclusion

In this paper, we propose a wavelet-based watermarking technique by adaptively quantizing a pair of family trees. The family trees are created by a group of wavelet coefficients of the different decomposition levels along the same spatial directions. Each watermark bit is embedded in various frequency bands and therefore is spread across large spatial regions. As a result, the watermark technique is robust against the common image processing attacks. Our extensive experimental results also demonstrate that our proposed system has the comparable performance as the fixed quantization approach and resist the common image processing attacks. The major contributions consist of:

- Adaptive HVS-based maximum allowable quantization error computation.
- Robust and adaptive quantization based watermarking embedding in DWT domain.
- Robust and blind quantization based watermarking detection in DWT domain.

References

- [1] G. C. Langelaar, I. Setyanwn, & R. L. Lagendijk, Watermarking digital image and video data, a state-of-the-art overview, *IEEE Signal Processing Magazine*, 2000, 20-46.
- [2] Reza Safabakhsh, Shiva Zaboli, & Arash Tabibiazar, Digital watermarking on still images using wavelet transform, *Proc. IEEE Conf. on Coding and Computing (ITCC'04)*, 2004, xx-xx.
- [3] I. Cox & M. L. Miller, A review of watermarking and the importance of perceptual modeling, *Proc. Electronic Imaging*, 1997, xx-xx.
- [4] A. H. Tewfik & M. Swanson, Data hiding for multimedia personalization, interaction, and protection, *IEEE Signal Processing Magazine*, 14, 1997, 41-44.
- [5] R. B. Wolfgang, C. I. Podilchuk, & E. J. Delp, Perceptual watermarks for digital images and video, *Proc. IEEE*, 87, 1999, 1108-1126.
- [6] S. Craver, N. Memon, B. Yeo, & M. Yeung, Resolving rightful ownerships with invisible watermarking techniques: Limitations, attacks, and implications, *IEEE J. Select. Areas Communications*, 16(X), 1998, 573-586.
- [7] I. J. Cox, J. Kilian, F. T. Leighton, & T. Shamoan, Secure spread spectrum watermarking for multimedia, *IEEE Trans. Image Processing*, 6, 1997, 1673-1687.
- [8] H. J. M. Wang, P. C. Su, & C. C. J. Kuo, Wavelet-based digital image watermarking, *Opt. Express*, 3(12), 1998, 491-496.
- [9] M. Barni, F. Bartolini, & A. Piva, Improved wavelet-based watermarking through pixel-wise masking, *IEEE Trans. Image Processing*, 10(5), 2001, 783-791.
- [10] D. Kundur & D. Hatzinakos, A robust digital image watermarking method using wavelet-based fusion, *Proc. 4th IEEE Int. Conf. Image Processing*, Santa Barbara, CA, 1997, 544-547.
- [11] C. T. Hsu and J. L. Wu, Multiresolution watermarking for digital images, *IEEE Trans. on Circuits Syst. II*, 45, 1998, 1097-1101.
- [12] M. S. Hsieh, D. C. Tseng, & Y. H. Huang, Hiding digital watermarks using multi-resolution wavelet transform, *IEEE Trans. Industrial Electronics*, 48(5), 1002, 875-882.
- [13] D. Kundur & D. Hatzinakos, Digital watermarking using multiresolution wavelet decomposition, *Proc. IEEE ICASSP*, 5, 1998, 2969-2972.
- [14] S. H. Wang & Y. P. Lin, Wavelet tree quantization for copyright protection watermarking, *IEEE Trans. on Image Processing*, 13(2), 2004, 154-165.
- [15] A. S. Lewis & G. Knowles, Image compression using the 2D wavelet transform, *IEEE Trans. on Image Processing*, 1, 1992, 244-250.